Brazilian Journal
of Chemical
Engineering

ISSN 0104-6632
Printed in Brazil
www.abeq.org.br/bjche

Vol. 31, No. 02, pp. 519 - 529, April - June, 2014
dx.doi.org/10.1590/0104-6632.20140312s00002103

ADSORPTION OF LEAD AND COPPER IONS FROM AQUEOUS EFFLUENTS ON RICE HUSK ASH IN A DYNAMIC SYSTEM

M. G. A. Vieira[1*], A. F. de Almeida Neto[1*], M. G. C. da Silva[1],
C. N. Carneiro[2] and A. A. Melo Filho[2]

[1]Department of Products and Processes Design, Phone: + (55) 19 35213895, Fax: + (55) 19 35213965,
University of Campinas, UNICAMP, 13083-852, Campinas - SP, Brazil.
[*]E-mail: melissagav@feq.unicamp.br
[*]E-mail: ambrosio@feq.unicamp.br; meuris@feq.unicamp.br
[2]Department of Chemistry, Federal University of Roraima, Boa Vista - RR, Brazil.
E-mail: candicenobrega@gmail.com; antonioalvesufrr@gmail.com

(Submitted: July 10, 2012 ; Revised: July 5, 2013 ; Accepted: August 8, 2013)

Abstract - This study evaluated the kinetic adsorption of Pb and Cu ions using rice husk ash as adsorbent in a fixed bed. The maximum adsorption capacities obtained for lead and copper ions in the fixed bed were 0.0561 and 0.0682 mmol/g (at 20 °C), respectively. The thermodynamic studies indicated that the lead adsorption process was exothermic and spontaneous, while the copper adsorption process was endothermic and spontaneous. Characterization results indicated the presence of several functional groups, amorphous silica and a fibrous and longitudinal structure of rice husks. Rice husk ash (RHA) from northern Brazil can be used as a bioadsorbent for the individual removal of Pb(II) and Cu(II) ions from metal-containing effluents.

Keywords: Adsorption; Heavy metal removal; Rice husk ash.

INTRODUCTION

Agricultural residues, especially rice husk, are by-product of the rice milling industry, being produced in large quantities as a waste, creating environmental problems.

Rice husk is mostly used as a fuel in the boiler furnaces of various industries to produce energy. The ash generated after burning the rice husk in the boiler is called rice husk ash. The rice husk ash was collected from the particulate collection equipment attached upstream to the stack of rice-fired boilers. The ash generated represents a severe disposal problem (Naiya *et al*., 2009; Srivastava *et al*., 2006).

Rice husk consists mainly of crude protein (3%), ash (including 17% silica), lignin (20%), hemicellulose (25%), and cellulose (35%), rendering it suitable for metallic cation fixation (Krishnani *et al*., 2008).

Today, heavy metals are the most serious pollutants, becoming an extreme public health problem. Processes such as chemical precipitation, solvent extraction, ion exchange, reverse osmosis or adsorption are commonly carried out with the aim of removing heavy metals, metalloid species, and their compounds from aqueous solution. Among these processes, the adsorption process is a simple and effective technique for the removal of heavy metals from wastewater (Ahmaruzzaman, 2010).

A number of materials have been widely investigated as adsorbent in water pollution control. Some of the important ones include zeolites (Wang and Peng, 2009; Okolo *et al*., 2000), activated carbon

---

*To whom correspondence should be addressed

(Wahby *et al*., 2011; Moreno-Pirajáń *et al*., 2011; Attia *et al*., 2010; Giraldo and Moreno-Pirajáń, 2008), rubber ash (Mousavi *et al*., 2010), clay (Galindo *et al*., 2013; Almeida Neto *et al*., 2012; Vieira *et al*., 2010a; Vieira *et al*., 2010b), expanded perlite (Torab-Mostaedi *et al*., 2010), vermiculite (Nishikawa *et al*., 2012), algae (Vieira *et al*., 2008; Vijayaranghavan *et al*., 2005; Silva *et al*., 2003), bacteria (Yilmaz *et al*., 2010), coir pith (Parab *et al*., 2006), sugarcane bagasse (Lv *et al*., 2008; Gupta and Ali, 2004), olive stone (Calero *et al*., 2009) and rice husks (Vieira *et al*., 2012; Vieira *et al*., 2011; Senthil Kumar *et al*., 2010; Naiya *et al*., 2009; Srivastava *et al*., 2006; Ye *et al*., 2010; Nakbanpote *et al*., 2007; Tarley and Arruda, 2004; Tarley *et al*., 2004).

In this context, adsorption of copper and lead from aqueous solution were evaluated using this potential material, through kinetic and thermodynamic studies in batch and fixed bed. Mathematical models were used to investigate the adsorption kinetics in batch and fixed bed. Langmuir and Freundlich's isotherm equations were applied to the experimental data. The adsorbent was characterized before and after the lead and cooper adsorption process.

MATERIALS AND METHODS

Adsorption

Samples of *Oryza sativa L.* rice husks from the North region of Brazil were used for adsorption. The rice husks were triturated in a food processor and calcined at 500 °C in a muffle furnace for one hour.

Metal Adsorbate and Chemical Speciation

The adsorption experiments were conducted using an aqueous solutions of $Cu(NO_3)_2.3H_2O$ and $Pb(NO_3)_2$ at a fixed concentration. The Cu(II) and Pb(II) solution pH was maintained at a level below minimal precipitation in order to assure the exclusive occurrence of the adsorption process and no chemical precipitation of copper and lead ions in the oxide and hydroxide forms (CuO and $Pb(OH)_2$), respectively. The effect of pH was estimated with HYDRA (Puigdomenech, 2004). The chemical precipitation of copper and lead in aqueous solution as oxide and hydroxide (CuO and $Pb(OH)_2$), respectively, occurs in the pH range of 5.0-12.0. Thus, the pH of the adsorbate solution was kept to 4.5 to ensure minimal precipitation on the adsorbent surface, thus making the adsorption of charged metal ions more favorable. The pH of the metal adsorbate solution was measured with a pH-meter with automatic temperature compensation, and maintained it at the proper value using nitric acid and ammonium hydroxide.

Column Sorption Procedure

Copper and lead adsorption runs in the dynamic system were performed in a glass column with internal diameter of 1.4 cm and 14.0 cm in height. The bed height used in the experiments was 14.0 cm. Before the runs, the rice husk ashes were deposited inside the column and put in contact with deionized water for 2 hours.

The solutions containing the metal species were fed at the base of the column through a peristaltic pump (Masterflex) at a constant flow rate defined by preliminary tests in which the mass transfer zone (MTZ) for lead was obtained. Column effluent samples were collected at time intervals pre-set by a FC203 fraction collector (Gilson).

The amounts of metal retained in the bed from the point of rupture (q_u) until saturation (q) were obtained by mass balance using column saturation data from the breakthrough curves. The area under the curve (1-C/C_0) to the breaking point is proportional to q_u and to exhaustion of the bed is proportional to q. The amounts retained were calculated from Eqs. (1 – 2), respectively.

$$q_u = \frac{C_0 V}{1000m}\int_0^{t_b}(1-\frac{C|_{Z=L}}{C_0})dt \qquad (1)$$

$$q = \frac{C_0 V}{1000m}\int_0^{\infty}(1-\frac{C|_{Z=L}}{C_0})dt \qquad (2)$$

The MTZ can then be calculated based on the q_u/q ratio according to Eq. (3) (Geankoplis, 1993):

$$\mathrm{MTZ} = \left(1-\frac{q_u}{q}\right)\cdot \mathrm{Ht} \qquad (3)$$

The MTZ has a maximum value which corresponds to the bed height (Ht). As the efficacy of mass transfer increases, this value decreases until reaching the ideal condition where the MTZ is zero and the breakthrough curve is a step function.

The percentage of total removal (%Rem) during adsorption was obtained by considering the metal fraction in solution retained in the adsorbent solid, from the total effluent used in the adsorption process until bed saturation. The amount of adsorbed metal was calculated by considering the curve area ($1-C/C_0$) versus t. The integral of the metal adsorption curves was determined with the software Origin® version 6.0.

Adsorption Thermodynamics

The adsorption experiments were performed using aqueous solutions of $Cu(NO_3)_2$ and $Pb(NO_3)_2$ of fixed concentrations in batch mode, at room temperature and under constant stirring of 225 rpm. At equilibrium times of 1000 and 600 min for removal of lead and copper, respectively (Vieira *et al.*, 2012), 4 mL-aliquots of the metal ion solutions were removed and centrifuged. The supernatant liquid was diluted and its concentration was determined by atomic absorption spectrometry (Perkin Elmer AA Analyst 100 with air-acetylene oxidizing flame). Removal capacity in the solid phase (q) at each time was obtained by Eq. (4):

$$q(t) = \frac{V}{m}\left(C_0 - C(t)\right) \tag{4}$$

The pH of the solutions defined by metallic speciation was 4.0 for Pb and 4.5 for Cu. The pH of the solutions was adjusted using 0.2 M HNO_3 or 0.25 M NH_4OH. Thermodynamic parameters for the adsorption process (ΔH (kJ/mol), ΔS (J/mol.K) and ΔG (kJ/mol)) were evaluated using the thermodynamic Eqs. (5) - (6).

$$\Delta G = -RT.\ln K_d \tag{5}$$

$$\ln(K_d) = -\Delta G/RT = \Delta S/R - \Delta H/RT \tag{6}$$

The graph of $\ln(K_d)$ *versus* 1/T must be linear with slope ($-\Delta H/R$) and intercept on the y axis of ($\Delta S/R$), providing the ΔH and ΔS values. The Gibbs Free Energy variation (ΔG) is the fundamental criterion of process spontaneity. A given process occurs spontaneously at a given temperature if $\Delta G < 0$.

Mathematical Model of the Adsorption Column

Bohart and Adams (1920) developed one of the simplest models to represent the breakthrough curve. This model assumes that the adsorption rate is proportional to the residual capacity for adsorption and concentration of the adsorbed species, and does not consider it to be important to stress the axial dispersion. In this case the intraparticle diffusion is negligible. The mass transfer rates satisfy Eqs. (7) and (8):

$$\frac{\partial C}{\partial t} + \frac{\rho_L}{\varepsilon}\frac{\partial q}{\partial t} + \nu\frac{\partial C}{\partial z} = 0 \tag{7}$$

$$\frac{\partial q}{\partial t} = kC(q_s - q) \tag{8}$$

where z is the height of the bed, v the flow velocity, ε is the porosity of the bed, ρ_L is the density of the bed, t is the process time and the parameters k, represent the constant removal rate.

The choice of this model is due to the fact that it assumes that the removal capacity is constant and that the isotherms obtained for the adsorbents show irreversible behavior. Thus, for a better representation of this study we used the sorption capacity of the adsorbent as the amount of metal removed when the system is in equilibrium. The initial boundary conditions are represented by Eqs. (9) and (10):

$$C(0,z) = 0 \text{ and } q(0,z) = 0 \tag{9}$$

$$C(t,0) = \begin{cases} 0 & \Leftrightarrow t = 0 \\ C_0 & \Leftrightarrow t > 0 \end{cases} \tag{10}$$

The analytical solution of the model of Adams and Bohart is given by Eq. (11), as shown by Ruthven (1984):

$$\frac{C}{C_0} = \frac{e^{\tau}}{e^{\tau} + e^{\xi} - 1} \tag{11}$$

where:

$$\tau = kC_0\left(t - \frac{z}{v}\right) \tag{12}$$

$$\xi = \frac{kq_0 z}{v}\left(\frac{1-\varepsilon}{\varepsilon}\right) \tag{13}$$

and q_0 represents the *quasichemical* concentration of metal in the solid state at time zero of the elution.

Adsorbent Characterization

The physical–chemical characterization of rice husk included morphological analysis by scanning electron microscopy (SEM) with EDX and Fourier-transform infrared spectroscopy (FTIR). The above mentioned analyses were performed for samples of rice husks *in natura*, calcined and after metal ion adsorption. Table 1 shows the analyses and their respective equipment.

Table 1: Characterization analysis of rice husk.

Analysis	Equipment	Parameters/observations
Fourier-transform infrared spectroscopy (FTIR)	Spectrum One—FT-IR, PerkinElmer	IR adsorption spect ra were obtained in KBr disks in the 4000–400 cm^{-1} region
Scanning electron microscopy (SEM)	SEM, model LEO 440i	Vacuum drying (12 h); metallization of samples with gold, utilizing 1V voltage and 3 nA current for 180 s, in an argon atmosphere

RESULTS AND DISCUSSION

Determination of the Operating Flow Rate for Fixed Bed Adsorption

The determination of the operating flow rate was based on the Mass Transfer Zone (MTZ). The concentration of adsorbate metal solution was kept constant at 0.48 mmol/L and 1.57 mmol/L for lead and copper, respectively, while the feed flow rate varied from 2, 3, 4 and 5 mL/min. Figure 1 shows the breakthrough curves at different flow rates in the adsorption of lead and copper. The experimental data were fit by the quasichemical solution function.

From Figure 1, it appears that the breakthrough curves present different behaviors, indicating the influence of diffusional resistances. The adsorption process has a strong resistance to the saturation of the bed in the entire flow range investigated, as evidenced by the more elongated breakthrough curves and the large areas of the mass transfer zone.

According to Geankoplis (1993), the mass transfer zone (MTZ) represented by the curve delineates a rupture length of the bed in which the concentration is given from the breaking point until the point of exhaustion. The shorter the length of the MTZ, the closer the system is to ideality, indicating a low diffusional resistance, and hence a more favorable adsorption process.

In the fixed bed adsorption process, when the flow rate is increased, the resistance to mass transfer in the liquid film outside is reduced; consequently, the mass transfer zone (MTZ) is reduced, as observed by Vijayaranghavan *et al.* (2005). However, using higher flow rates, the MTZ is increased, because the fluid does not have a residence time sufficient for the adsorption to occur. Table 2 shows the values of MTZ, q_u, q and percentage removal (%Rem) of lead and copper in RHA.

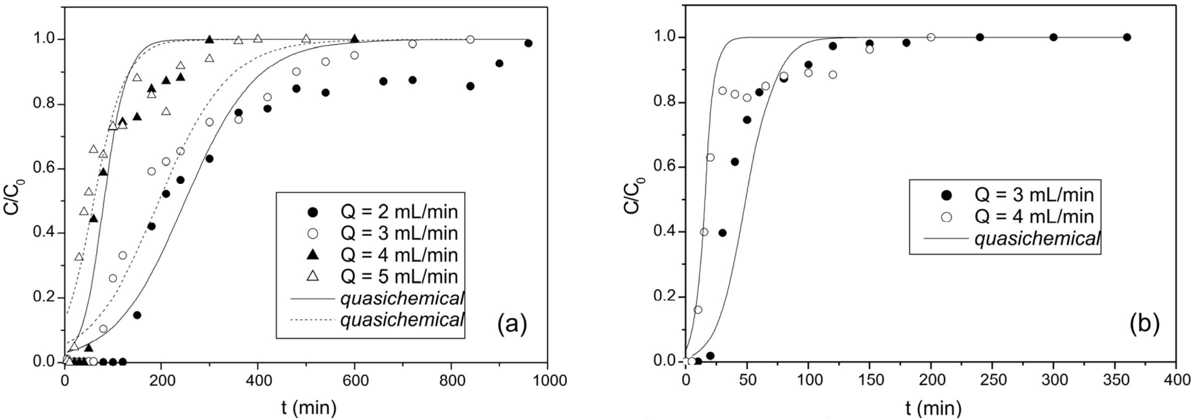

Figure 1: Breakthrough curves for the system: (a) Pb^{2+}/RHA, (b) Cu^{2+}/RHA at different flow rates, 0.48 mmol / L of lead and 1.57 mmol / L copper in solution, adjusted by the function *quasichemical*.

Table 2: Values of the MTZ, q_u and q for the adsorption removal of lead and copper by RHA.

System	Flow (mL/min)	MTZ (cm)	q_u (mmol/g)	q (mmol/g)	%Rem
Pb^{2+}/RHA	2	9.08	0.0227	0.0575	33.33
	3	10.64	0.0185	0.0636	31.33
	4	8.22	0.0239	0.0529	33.05
	5	12.35	0.01	0.0561	23.23
Cu^{2+}/RHA	3	9.12	0.0166	0.0423	17.08
	4	11.18	0.0137	0.0682	22.22

Table 2 shows that the lowest values of MTZ and satisfactory values of useful (q_u) and total amount of metal adsorbed (q) and percentage of total removal (%Rem) were obtained at a flow rate of 4 mL/min for both ions. The values of q_0 and k are presented in Table 3. The parameter q_0 was only little influenced by changes in the flow rate. This can be attributed to the constant number of sites used by lead or copper during the adsorption process. The parameter k varies with the increase of the operating flow rate. For each operating flow rate, a new breakthrough curve is established.

Thermodynamics of Adsorption

Thermodynamic data were obtained through the static method in a thermostated bath with constant stirring (225 rpm) at various temperatures (24 - 74 ºC). An increase in temperature increases the adsorption capacity, which means that the increase of energy favours adsorption on the RHA surface. Pb/RHA presents a negative enthalpy variation during adsorption (exothermic process). Naiya *et al.* (2009) obtained results that indicated that the Pb removal degree increases with an increase in temperature for an initial concentration of 50 ppm, pH 5.0, and contact time of 1 hour, using RHA as adsorbent: for 30 ºC, they obtained 94.85%; for 40 ºC, 95.30%; and for 50 ºC, 96.02% of metal removal.

Figure 2 shows adsorption isotherms for 1g RHA/ 100 mL of adsorbate solution. The equilibrium data were adjusted by Langmuir and Freundlich's models. The initial concentration of Pb varied from 5 to 800 ppm for the four temperature levels and the initial concentrations of Cu varied from 5 to 500 ppm for the three temperature levels.

The parameters obtained from the Langmuir and Freundlich models and Henry's constants are presented in Table 4. Figure 2 and Table 4 show that Langmuir's model better represented the experimental data for the adsorption isotherms.

Table 3: Quasichemical solution fit for breakthrough curves.

System	Flow (mL/min)	q_0	k	R^2
Pb^{2+}/RHA	2	52.7899	0.0289	0.9592
	3	66.2056	0.0285	0.9493
	4	53.3139	0.0918	0.9350
	5	52.9429	0.0633	0.8811
Cu^{2+}/RHA	3	45.7012	0.0610	0.9215
	4	30.5621	0.1005	0.8512

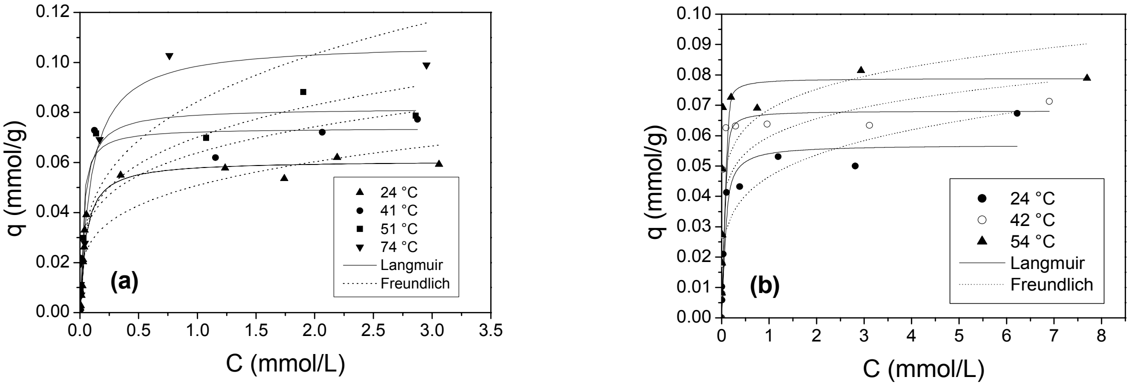

Figure 2: Langmuir and Freundlich isotherms for (a) lead and (b) copper on RHA.

Table 4: Adsorption isotherm parameters for the removal of Pb and Cu ions.

System	T(K)	Langmuir			Freundlich			Henry	
		q_m (mmol/g)	b (L/g)	R^2	A	n	R^2	K (L/g)	R^2
Pb/RHA	297	0.0608	19.3743	0.9628	0.0508	0.2471	0.8202	0.7752	0.9152
	314	0.0738	45.1749	0.9277	0.0638	0.2191	0.7909	0.5262	0.9202
	324	0.0818	27.2375	0.9698	0.0701	0.2420	0.8611	0.4795	0.9276
	347	0.1080	10.3973	0.9809	0.0843	0.2932	0.8517	0.3835	0.9359
Cu/RHA	297	0.0570	18.4312	0.9397	0.0465	0.2060	< 0.9	0.3875	0.9625
	315	0.0682	55.5226	0.9305	0.0596	0.1369	< 0.9	1.7405	0.9915
	327	0.0789	70.4091	0.9178	0.0686	0.1342	< 0.9	2.7481	0.9675

The Langmuir-Freundlich is a versatile isotherm expression that can represent both Langmuir and Freundlich behaviours. A general form of the Langmuir-Freundlich isotherm equation for copper and lead adsorption on RHA can be written as Eq. (14):

$$q = \frac{Q_m (K_a C_{eq})^n}{(K_a C_{eq})^n + 1} \tag{14}$$

where, q is the amount of metal adsorbed on the ash at equilibrium (mmol/g), Q_m is the adsorption capacity of the system (mmol of adsorbate/g adsorbent), C_{eq} is the aqueous phase concentration at equilibrium (mmol/ L), K_a is the affinity constant for adsorption (L/g) and n is the index of heterogeneity

The Langmuir-Freundlich isotherm was fitted to all isotherm datasets as shown in Figure 3. The fitted values of Q_m, K_a and n are summarized in Table 5. The parameter estimation process was robust and the *Origin* solver converged to these parameter values for a wide range of initial conditions. The only restriction used in the solver was a non-negativity constraint for the K_a values. The R^2 values of the fitting were greater than 0.92. These results indicate that the Langmuir-Freundlich isotherm can be used to describe temperature effects on lead and copper adsorption.

The thermodynamic parameters obtained are presented in Table 6. Pb/RHA interactions occurred spontaneously (ΔG<0) and the adsorption process is exothermic. Spontaneity increases with the rise in temperature, varying from -17.243 to -18.156 kJ/mol for the temperature range of 24 to 74 ºC. The Cu/RHA interactions also occurred spontaneously (ΔG<0), but the adsorption process is endothermic. Similar results were obtained by different authors, who also verified an endothermic behaviour for adsorption of copper ions on several clays (Bhattacharyya and Gupta, 2008; Eren and Afsin, 2008; Bhattacharyya and Gupta, 2007; Weng *et al.*, 2007). Thus, the adsorption of Cu(II) onto clays has to overcome a small activation energy barrier and an increase in energy supply makes it easier for Cu(II) to adsorb onto the clay surface. Such activated adsorption following an endothermic path has also been reported earlier (Futalan *et al.*, 2011).

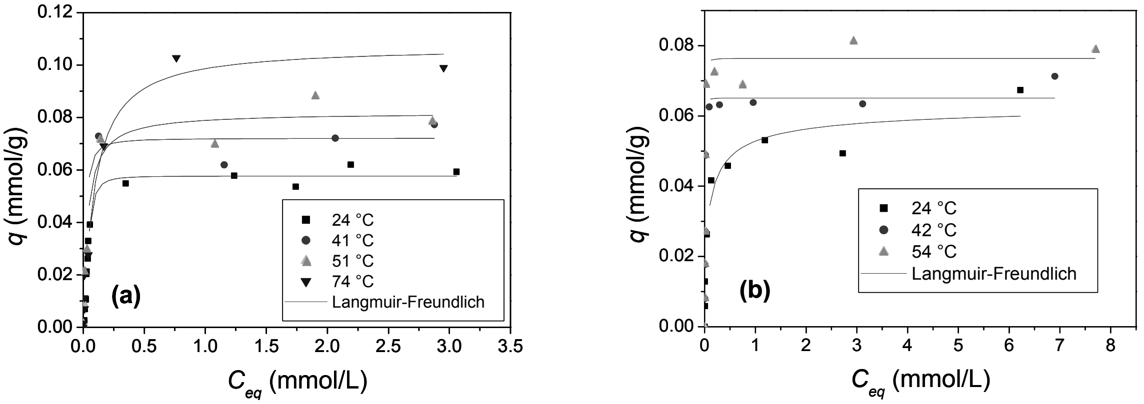

Figure 3: Langmuir-Freundlich isotherms for (a) lead and (b) copper on RHA.

Table 5: Langmuir-Freudlich isotherm parameters for the removal of Pb and Cu ions.

System	Langmuir-Freundlich				
	T (K)	Q_m	K_a	n	R^2
Pb/RHA	297	0.058	787.2	1.043	0.988
	314	0.072	264.6	0.398	0.920
	324	0.082	26.37	0.008	0.965
	347	0.107	11.72	0.039	0.979
Cu/RHA	297	0.064	4.7	0.383	0.928
	315	0.065	56.5	1.591	0.952
	327	0.076	15.8	1.241	0.948

Table 6: Thermodynamics parameters for Pb(II) and Cu(II) adsorption on RHA.

System	Δ*H* (kJ/mol)	Δ*S* (J/mol K)	Δ*G* (kJ/mol)			
			297 K	314 K	324 K	347 K
Pb/RHA	-11.82	+18.26	-17.243	-17.554	-17.736	-18.156
Cu/RHA			297 K	315 K	327 K	--
	+53.95	+235.05	-15.859	-20.091	-22.911	--

Characterization

FTIR Analysis

The FTIR technique is an important tool to identify characteristic functional groups. In Figure 4(a) and (b), note the presence of OH groups on the sample surface (Kamath and Proctor, 1998). This OH stretching is due to silanol groups (Si-OH). Besides, a methyl group has been identified. Stretches due to the presence of lignin (Tarley *et al.*, 2004), aldehydes and ketones, aromatic rings (Tarley and Arruda, 2004) and siloxane (Si-O-Si) (Nakbanpote *et al.*, 2007; Tarley and Arruda, 2004; Tarley *et al.*, 2004) groups in the samples are also present. Table 7 shows the functional groups and their respective wavelengths identified in the spectra.

Scanning Electron Microscopy

Figure 5 presents SEM micrographs of the rice husks and rice husk ash before and after adsorption. SEM micrographs of the rice husk ash (5b) indicated that the surface was highly irregular and porous *in nature* (Naiya *et al.*, 2009). The cob-shaped cellulose skeleton is visible (Della *et al.*, 2001). According to Della *et al.* (2001), the inner epidermis presents a pore structure resulting from removal of lignin and cellulose during the burning process; cellulose is the major organic constituent of rice husks. Based on the mapping of metals in the micrographs performed by EDX it is possible to observe a uniform distribution of the metallic ions lead (Figure 5c) and copper (Figure 5d) on the RHA surface after adsorption.

According to Tarley and Arruda (2004), the morphology of the adsorbent can facilitate adsorption of metals in different parts of the material. Therefore, based on morphology and on the fact that a higher concentration of silica is present in the outer epidermis of the rice hulls, one can conclude that this material presents a morphological profile with the capability to retain metal ions.

The semi-quantitative chemical composition obtained by EDX (coupled to SEM) of the compounds in RHA is shown in Table 8. Ion exchange can be an additional process for removal of copper and lead by RHA, being verified by the results of chemical composition presented in Table 8, where the percentage of exchangeable potassium in the RHA drastically decreased after adsorption. The mechanism of ion exchange can be written as follows:

$$2K^+ - RHA + Cu^{2+} \rightarrow Cu^{2+} - RHA + 2K^+$$

$$2K^+ - RHA + Pb^{2+} \rightarrow Pb^{2+} - RHA + 2K^+$$

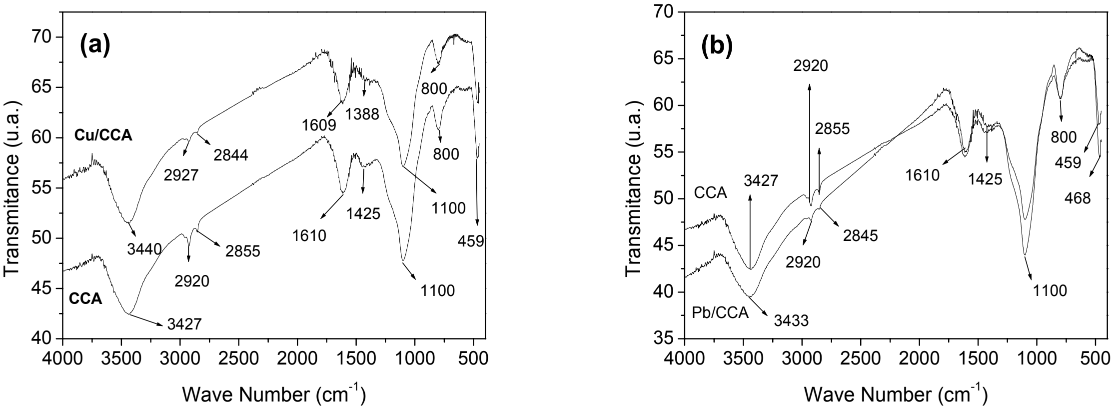

Figure 4: FTIR spectra of (a) RHA and Cu/RHA, (b) RHA and Pb/RHA.

Table 7: Absorption bands identified in the FTIR Spectra.

RHA Wavelength (cm^{-1})	Cu/RHA Wavelength (cm^{-1})	Pb/RHA Wavelength (cm^{-1})	Functional Groups
3427	3440	3433	-OH
2920 and 2855	2927 and 2844	2920 and 2845	CH_3
1610	1609	1610	-C=O
1425	1388	1425	Aromatic rings
1100	1100	1100	Si-O-Si
800 and 459	800 and 468	800 and 468	N-H

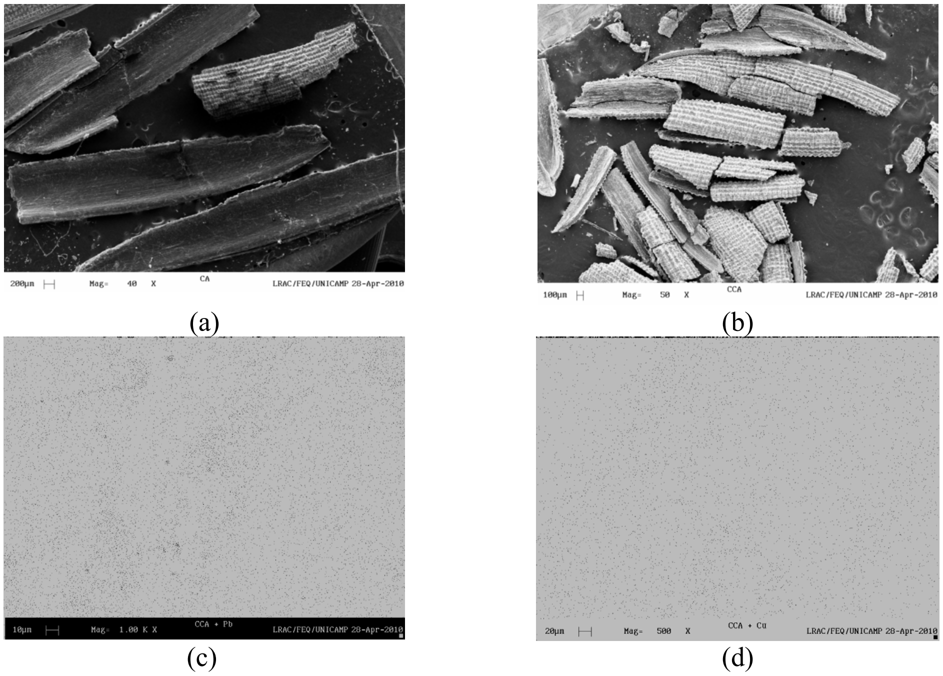

Figure 5: SEM micrographs: (a) Rice husk inner and outer epidermis with 50x magnification; (b) Rice husk ash inner and outer epidermis with 200X magnification; (c) Pb/RHA with 1000x magnification; (d) Cu/RHA with 500x magnification.

Table 8: Chemical analysis of the RHA.

Sample	**Composition (%)**						
	O	**Si**	**K**	**Ca**	**Cu**	**Pb**	**Sum**
RHA	52.45	45.59	1.40	0.56	--	--	100
RHA + Cu	58.90	37.56	0.53	1.37	1.64	--	100
RHA + Cd	55.20	43.77	0.45	0.28	--	0.30	100

Similar results were obtained by Galindo *et al.* (2013) in a study of the removal of cadmium and lead using sodic clay. The authors reported that ion exchange can be an additional process for removal of cadmium and lead on sodic clay and that the amount of exchangeable cations Na^+ was reduced after metal adsorption.

CONCLUSIONS

The study of mass transfer parameters, as well as the breakthrough curves, indicated that the most suitable operating flow rate, i.e., which minimizes the diffusional resistances in the bed for removal of lead and copper by RHA was 4 mL/min. When the flow rate was increased, the breaking and the saturation points, as well as the useful (q_u) and the total (q) amount of metal adsorbed decreased. RHA from northern Brazil can be used as a bioadsorbent for the individual removal of Pb(II) and Cu(II) ions from metal-containing effluents and the maximum sorption found for both ions was 0.0561 and 0.0682 mmol metal/g of RHA, respectively. The thermodynamic study indicated that the Pb adsorption process was exothermic and spontaneous, while Cu adsorption was endothermic and spontaneous. Sorption isotherms were well-described by Langmuir's model. The physical characterization of rice husks in nature, rice husk ash before and after adsorption of metal ions pointed to properties such as the presence of functional groups (carboxyl, silanol, hydroxyl, etc.), of amorphous silica and of a fibrous and longitudinal structure of this material.

NOMENCLATURE

a, n	Freundlich coefficients
b, q_m	Langmuir coefficients representing the equilibrium constant for the adsorbate–

	adsorbent equilibrium and the maximum adsorbed amount on the monolayer	
C	metal concentration in a solution in the column outlet	ppm
C_0	initial metal concentration in the liquid	ppm
K	Henry constant	
K_d	adsorbate distribution coefficient	$=q_{eq}/C_{eq}$ L/g
Q	amount of adsorbed metal per unit of adsorbent mass	mg of metal/g of adsorbent
q_u	amount of adsorbed metal per unit of adsorbent mass up to the breakthrough point	mg of metal/g of adsorbent
R	universal gas constant	8.314×10^{-3} kJ/(K mol)
T	temperature	K
t_b	time until breakthrough point	min
V	volumetric outflow of the metal solution	cm^3/min
ΔG	Gibbs free energy variation	kJ/mol
ΔH	enthalpy variation	kJ/mol
ΔS	entropy variation	J/(K mol)

REFERENCES

Ahmaruzzaman, M., A review on the utilization of fly ash. Prog. Energy Combust. Sci., 36, 327-363 (2010).

Almeida Neto, A. F. de, Vieira, M. G. A. and Da Silva, M. G. C., Cu(II) adsorption on modified bentonitic clays: Different isotherm behaviors in static and dynamic systems. Mater. Res., 15, 114-124 (2012).

Attia, A. A., Khedr, S. A. and Elkholy, S. A., Adsorption of chromium ion (VI) by acid activated carbon. Braz. J. Chem. Eng., 27(1), p. 183-193 (2010).

Bhattacharyya, K. G. and Gupta, S. S., Adsorption of a few heavy metals on natural and modified kaolinite and montmorillonite: A review. Adv. Colloid Interface Sci., 140, 114-131 (2008).

Bhattacharyya, K. G. and Gupta, S. S., Adsorptive accumulation of Cd(II), Co(II), Cu(II), Pb(II), and Ni(II) from water on montmorillonite: Influence of acid activation. J. Colloid Interface Sci., 310, 411-424 (2007).

Calero, M., Hernáinz, F., Blázquez, G., Martín-Lara, M. A. and Tenorio, G., Biosorption kinetics of Cd (II), Cr (III) and Pb (II) in aqueous solutions by olive stone. Braz. J. Chem. Eng., 26(2), p. 265-273 (2009).

Della, V. P., Kuhn, I. and Hotza, D., Characterization of rice husk ash for use as feedstock in the manufacture of silica refractories. Quim. Nova, 24, 778-782 (2001). (In Portuguese).

Eren, E. and Afsin, B., An investigation of Cu^{2+} adsorption by raw and acid-activated bentonite: A combined potentiometric, thermodynamic, XRD, IR, DTA study. J. Hazard. Mater., 151, 682-691 (2008).

Futalan, C. M., Kan, C.-C., Dalida, M. L., Hsien, K.-J., Pascua, C. and Wan, M.-W., Comparative and competitive adsorption of cooper, lead and nickel using chitosan immobilized on bentonite. Carbohyd. Polym., 83, 528-536 (2011).

Galindo, L. S. G., Almeida Neto, A. F. de, Silva, M. G. C., Vieira, M. G. A., Removal of cadmium(II) and lead(II) ions from aqueous phase on sodic bentonite. Mater. Res., 16, 515-527 (2013).

Geankoplis, C. J., Transport Process and Unit Operations. 3rd Ed. PTR Pretice Hall, USA (1993).

Giraldo, L. and Moreno-Piraján, J. C., Pb2+ adsorption from aqueous solutions on activated carbons obtained from lignocellulosic residues. Braz. J. Chem. Eng., 25(1), p. 143-151 (2008).

Gupta, V. K. and Ali, I., Remove of lead and chromium from wastewater using bagasse fly ash – a sugar industry waste. J. Colloid Interface Sci., 271, 321-328 (2004).

Ho, Y. S., Mckay, G., Wase, D. J. and Foster, C. F., Study of the sorption of divalent metal ions on to peat. Adsorpt. Sci. Technol., 18, 639-650 (2000).

Kamath, S. R. and Proctor, A., Silica gel from rice hull ash: Preparation and characterization. Cereal Chem., 75, 484-487 (1998).

Krishnani, K. K., Meng, X., Christodoulatos, C. and Boddu, V. M., Bisorption mechanism of nine different heavy metals onto biomatrix from rice husk. J. Hazard. Mater., 153, 1222-1234 (2008).

Krishnarao, R. V., Subrahmanyam, J. and Kumar, T. J., Studies on the formation of black particles in rice husk silica ash. J. Eur. Ceram. Soc., 21, 99-104 (2001).

Lagergren, S., Zur theorie der sogenannten adsorption geloster stoffe. Kungliga Svenska Vetenskapsakademiens, Handlingar (1898). (In Swedish).

Lv, Z., Yang, J., Wang, E. and Yuan, H., Characterization of extracellular and substrate-bound cellulases from a mesophilic sugarcane bagasse-degrading microbial community. Process Biochem., 43, 1467-1472 (2008).

Moreno-Piraján, J. C., Garcia-Cuello, V. S. and Giraldo, L., The removal and kinetic study of Mn, Fe, Ni and Cu ions from wastewater onto activated carbon from coconut shells. Adsorption, 17, 505-514 (2011).

Mousavi, H. Z., Hosseynifar, A., Jahed, V. and Dehghani, S. A. M., Removal of lead from aqueous solution using waste tire rubber ash as an adsorbent. Braz. J. Chem. Eng., 27(1), p. 79-87 (2010).

Naiya, T. K., Bhattacharya, A. K., Mandal, S. and Das, S. K., The sorption of lead(II) ions on rice husk ash. J. Hazard. Mater., 163, 1254-1264 (2009).

Nakbanpote, W., Goodman, B. A. and Thiravetyan, P., Cooper adsorption on rice husk derived materials studied by EPR and FTIR. Colloid, Surface, A, 304, 7-13 (2007).

Nishikawa, E., Almeida Neto, A. F. de, Vieira, M. G. A., Equilibrium and thermodynamic studies of zinc adsorption on expanded vermiculite. Adsorption Sci. Technol., 30, 759-772 (2012).

Okolo, B., Park, C. and Keane, M. A., Interaction of phenol and chlorophenols with activated carbon and synthetic zeolites in aqueous media. J. Colloid Interface Sci., 226, 308-317 (2000).

Parab, H., Joshi, S., Shenoy, N., Lali, A., Sarma, U. S. and Sudersanan, M., Determination of kinetic and equilibrium parameters of the batch adsorption of Co(II), Cr(III) and Ni(II) onto coir pith. Process Biochem., 41, 609-615 (2006).

Puigdomenech, I., HYDRA and MEDUSA Programs (Chemical Equilibrium Diagrams), Royal Institute of Technology, Sweden, software available at http://www.kemi.kth.se/medusa (2004).

Real, C., Alcalá, M. D. and Criado, J. M., Preparation of sílica from rice husks. J. Am. Ceram. Soc., 79, 2012-2016 (1996).

Ruthven, D. M., Principals of Adsorption and Adsorption Processes. John Wiley & Sons, USA (1984).

Senthil Kumar, P., Ramakrishnan, K., Dinesh Kirupha, S. and Sivanesan, S., Thermodynamic and kinetic studies of cadmium adsorption from aqueous solution onto rice husk. Braz. J. Chem. Eng., 27(2), p. 347-355 (2010).

Silva, E. A., Cossich, E. S., Tavares, C. G., Cardozo Filho, L., Guirardello, R., Biosorption of binary mixtures of Cr(III) and Cu(II) ions by Sargassum sp. Braz. J. Chem. Eng., 20(3), 213-227 (2003).

Srivastava, V. C., Mall, I. D. and Mishra, I. M., Characterization of mesoporous rice husk ash (RHA) and adsorption kinetics of metal ions from aqueous solution onto RHA. J. Hazard. Mater., 134, 257-267 (2006).

Tarley, C. R. T. and Arruda, M. A. Z., Biosorption of heavy metals using rice milling by-products. Characterization and application for removal of metals from aqueous effluents. Chemosphere, 54, 987-995 (2004).

Tarley, C. R. T., Ferreira, S. L. C. and Arruda, M. A. Z., Use of modified rice husks as a natura solid adsorbent of trace metals: characterization and development of an on-line preconcentration system for cadmium and lead determination by FAAS. Microchem. J., 77, 163-175 (2004).

Teng, H. and Wei, Y., Thermogravimetric studies on the kinectics of rice hull pyrolysis and the influence of water treatment. Indian Eng. Chem. Res., 37, 3806-3811 (1998).

Torab-Mostaedi, M., Ghassabzadeh, H., Ghannadi-Maragheh, M., Ahmadi, S. J. and Taheri, H., Removal of cadmium and nickel from aqueous solution using expanded perlite. Braz. J. Chem. Eng., 27(2), p. 299-308 (2010).

Vieira, M. G. A., Almeida Neto, A. F., Gimenes, M. L. and Da Silva, M. G. C., Sorption kinects and equilibrium for the removal of nickel ions from aqueous phase on calcined Bofe bentonite clay. J. Hazard. Mater., 177, 362-371 (2010a).

Vieira, M. G. A., Almeida Neto, A. F., Gimenes, M. L. and Da Silva, M. G. C., Removal of nickel on Bofe bentonite calcined clay in porous bed. J. Hazard. Mater., 176, 109-118 (2010b).

Vieira, M. G. A., Almeida Neto, A. F., Silva, M. G. C., Carneiro, C. N. and Melo Filho, A. A., Characterization and use of *in natura* and calcined rice husks for biosorption of heavy metals ions from aqueous effluents. Braz. J. Chem. Eng., 29, 619-633 (2012).

Vieira, M. G. A., Almeida Neto, A. F., Silva, M. G. C., Carneiro, C. N. and Melo Filho, A. A., Influence of the system on adsorption of Pb(II) and Cu(II) by rice husks ash: Kinetic study. Chem. Eng. Trans., 24, 1213-1218 (2011).

Vieira, M. G. A., Oisiovici, R. M., Gimenes, M. L. and Silva, M. G. C., Biosorption of Chromium (VI) using a sargassum sp packed-bed column. Bioresour. Technol., 99, 3094-3099 (2008).

Vijayaranghavan, K., Jegan, J., Palanivelu, K. and Velan, M., Biosorption of copper, cobalt and nickel by marine green alga Ulva reticulata in a packed column. Chemosphere, 60, 416-426 (2005).

Wahby, A., Abdelouahab-Reddam, Z., El Mail, R., Stitou, M., Silvestre-Albero, J., Sepúlveda-Escribano, A. and Rodríguez-Reinoso, F., Mercury removal from aqueous solution by adsorption on activated carbons prepared from olive stones. Adsorption, 17, 603-609 (2011).

Wang, S. and Peng, Y., Natural zeolites as affective adsorbents in water and wastewater treatment. Chem. Eng. J., 156, 11-24 (2010).

Weng, C.-H., Tsai, C.-Z., Chu, S.-H. and Sharma, Y. C., Adsorption characteristics of copper(II) onto spent activated clay. Sep. Purif. Technol., 54, 187-197 (2007).

Ye, H., Zhu, Q. and Du, D., Adsorptive removal of Cd(II) from aqueous solution using natural and modified rice husk. Bioresour. Technol., 101, 5175-5179 (2010).

Yilmaz, M., Tay, T., Kivanc, M. and Turk, H., Removal of corper(II) ions from aqueous solution by a lactic acid bacterium. Braz. J. Chem. Eng., 27(2), p. 309-314 (2010).